HHS Public Access

Author manuscript

Nat Chem. Author manuscript; available in PMC 2019 August 25.

Published in final edited form as:

Nat Chem. 2019 April ; 11(4): 335–341. doi:10.1038/s41557-019-0217-x.

Fluorogenic D-amino acids enable real-time monitoring of peptidoglycan biosynthesis and high-throughput transpeptidation assays

Yen-Pang Hsu[1], **Edward Hall**[2,5,*], **Garrett Booher**[1,*], **Brennan Murphy**[2,*], **Atanas D. Radkov**[2,6], **Jacob Yablonowski**[1], **Caitlyn Mulcahey**[1], **Laura Alvarez**[3], **Felipe Cava**[3], **Yves V. Brun**[4,†], **Erkin Kuru**[1,7,†], and **Michael S. VanNieuwenhze**[1,2,†]

[1]Department of Molecular and Cellular Biochemistry, Indiana University, Bloomington, IN 47405

[2]Department of Chemistry, Indiana University, Bloomington, IN 47405

[3]Department of Molecular Biology, Umeå University, Umeå, Sweden

[4]Department of Biology, Indiana University, Bloomington, IN 47405

[5]Current address: Department of Chemistry, Hanover College, Hanover, IN 47243

[6]Current address: Department of Biophysics and Biochemistry, University of California San Francisco, San Francisco, CA 94158

[7]Current address: Department of Genetics, Harvard Medical School, Boston, MA 02115

Abstract

Peptidoglycan (PG) is an essential cell wall component that maintains the morphology and viability of nearly all bacteria. Its biosynthesis requires periplasmic transpeptidation reactions which construct peptide cross-linkages between polysaccharide chains to endow mechanical strength. However, tracking transpeptidation reaction *in vivo* and *in vitro* is challenging, mainly due to the lack of efficient, biocompatible probes. Here, we report the design, synthesis, and application of rotor-fluorogenic D-amino acids (RfDAAs) enabling real-time, continuous tracking of transpeptidation reactions. These probes enable monitoring PG biosynthesis in real time through visualizing transpeptidase reactions in live cells, as well as real-time activity assays of D,D-, L,D-transpeptidases, and sortases *in vitro*. The unique ability of RfDAAs to become fluorescent when incorporated into PG provides a powerful new tool to study PG biosynthesis with

† Corresponding authors: Correspondence should be addressed to mvannieu@indiana.edu, erkin_kuru@hms.harvard.edu, and ybrun@indiana.edu.

*These authors contributed equally

Author Contributions

E.H., E.K. and Y.H. designed RfDAAs; Y.H., E.H., B.M., C.M. and J.Y. synthesized RfDAAs; Y.H. characterized RfDAAs; Y.H. and E.K. performed cell labeling and microscopy experiments; G.B., A.D.R., L.A.M. and F.C. prepared and performed the *in vitro* assays; Y.H., A.D.R., E.K., Y.V.B. and M.S.V. wrote the paper. All authors were involved in the design of this work.

Competing Interests

The authors declare no completing interests.

Data Availability

All data are available upon reasonable request to the corresponding authors.

high temporal resolution and prospectively enable high-throughput screening for inhibitors of PG biosynthesis.

Graphical Abstract

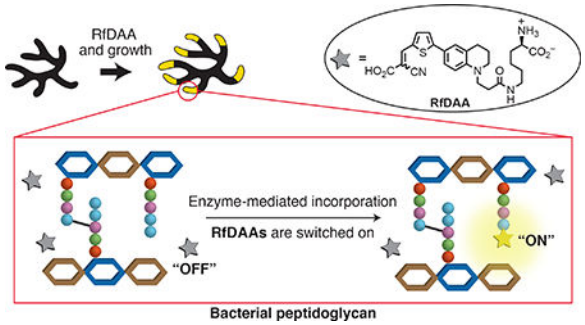

Peptidoglycan (PG) is a mesh-like macromolecule that surrounds the cytoplasmic membrane of nearly all bacteria, protecting them from environmental stress and dictating cell morphology throughout their life.[1–3] PG biosynthesis requires transpeptidation reactions for cross-linking PG glycan backbones via short peptide chains.[4] There are three types of transpeptidation reactions involved in PG biosynthesis: 1) D,D-transpeptidation constructs PG 3–4 crosslinks which are normally essential for bacterial viability. β-lactam antibiotics, such as penicillin, induce cytotoxicity via inhibition of D,D-transpeptidation catalyzed by penicillin-binding proteins (PBPs);[5–8] 2) L,D-transpeptidation produces PG 3–3 crosslinks and is conducted by L,D-transpeptidases (Ldts)[9]. Although Ldts are normally not essential in most species, their activities help cells bypass β-lactam toxicity in some bacteria;[10,11] and 3) sortase-catalyzed transpeptidation anchors surface proteins to the PG structure. Inhibition of sortase activity results in defective cell growth and infections in some species.[12,13]

Monitoring transpeptidation activity *in vivo* and *in vitro* remains challenging even though it has been studied for almost a century.[14] Previously, we reported the use of fluorescent D-amino acids (FDAAs) for PG labeling in various bacterial species.[15–19] FDAAs incorporate into PG peptide chains through D,D-transpeptidation and/or L,D-transpeptidation activity by enzyme-substrate mimicry.[4,15] Thus, FDAA labeling reflects transpeptidation reactions and allows direct observation of PG cross-linking activities. Nevertheless, continuous tracking of transpeptidase activities remains difficult. Sequential labeling using different colored FDAAs has been applied to study PG formation in real time, but the requirement of vigorous cell washing and lengthy harvest steps greatly reduces the temporal resolution of the experiments.[16,17,19] This requirement not only creates a time gap between the labeling pulses, but could also disturb the physiology of the cell. This, in turn, makes the interpretation of experiments involving highly dynamic process, e.g. the coordination of different PG synthases, difficult. Therefore, probes capable of continuous monitoring of PG transpeptidation activity with high temporal resolution and minimal cell disruption are in a great demand. These probes would allow in-depth elucidation of PG biosynthesis, providing new insights into bacterial propagation and its inhibition.

Fluorescent molecular rotors (FMRs) are a class of fluorophores whose emission intensity is sensitive to the ability of the environment to restrict bond rotation (or known as spatial hindrance).[20] In a low-hindrance environment, photo-excited FMRs adopt a twisted intramolecular charge transfer state (TICT) and release energy through red-shifted emission or non-radiative relaxation. Thus, no fluorescence signal is detected ("off state"). Under high spatial hindrance, conversion to the TICT state is inhibited, resulting in energy release through fluorescence emission ("on state"). The "on-off" property of FMRs has been classically used for measuring viscosity, but it has recently been applied to detect protein and DNA interactions as well.[21–26] Inspired by this property, we hypothesized that the incorporation of FMRs into PG, a congested environment, would be sufficient to provide a fluorogenic response.[24,27,28]

In this study, we report the first design and synthesis of three molecular rotor-fluorogenic DAAs (RfDAAs) and confirm their D,D- and L,D- transpeptidase-mediated incorporation into the PG layer of Gram-positive and Gram-negative bacteria. We show that end-point imaging of PG labeling can be carried out using RfDAAs without washing steps. Their "on-off" property enables, for the first time, time-lapse monitoring of PG growth in live cells. In addition, we demonstrate the use of the probes for *in vitro*, real-time activity assays of three types of transpeptidases. We evaluate the potential of RfDAA applications for a high-throughput transpeptidation assay that will significantly advance the studies of PG synthase mechanisms and kinetics analysis, as well as new antibiotic development.

Results

Synthesis of Rotor-fluorogenic DAAs (RfDAAs)

Fluorescent molecular rotors have been developed on several types of scaffolds, most notably benzonitrile and julolidine.[20,29] To enable cell labeling, we aimed to design RfDAAs having high water-solubility, stability, and biocompatibility. We started with a tetrahydroquinoline core whose derivatives showed molecular rotor properties and have been applied in studies under physiological conditions.[30] Synthesis was initiated with an N-alkylation of tetrahydroquinoline with methyl acrylate to create a linker for subsequent D-amino acid coupling (Fig. 1).[31] The resulting ester (**1**) was formylated through a Vilsmeier-Haack reaction, followed by ester hydrolysis to provide aldehyde **2**. Condensation with *t*-butyl cyanoacetate gave the molecular rotor **3**, which was coupled with D-lysine and deprotected to provide **Rf420DL** (**R**otor-**f**luorogenic **420 D-l**ysine).

Rf420DL possesses a maximum excitation wavelength (Max. λ_{Ex}) of 420 nm and a maximum emission wavelength (Max. λ_{Em}) of 490 nm (Table 1, Supplementary Fig. 1). Due to photo-toxicity concerns caused by low wavelength excitation, we inserted a thiophene group to the molecule to provide red-shifted $\lambda_{Ex}/\lambda_{Em}$ as previously reported by Shao *et al.*[32] Synthesis began with iodination to provide intermediate **4**. After ester hydrolysis, Suzuki-Miyaura coupling of thiophenyl aldehyde trifluoroborate was applied to generate intermediate **5**.[33,34] The synthesis was completed via condensation with *t*-butyl cyanoacetate (**6**), coupling with Boc-D-lysine, and final deprotection to give **Rf470DL**. **Rf470DL** has a max. λ_{Ex} of 470 nm (a red-shift of 50 nm compared to **Rf420DL**) and a max. λ_{Em} of 640 nm. Finally, to study the effect of molecular geometry on PG labeling, we

prepared a structural isomer of **Rf470DL**, called **Rf490DL**, where D-lysine is coupled to the vinyl carboxylate group instead of the N-alkyl linker. A red-shift of 20 nm was found in the Max. λ_{Ex} compared to **Rf470DL**.

RfDAAs enable end-point PG imaging without washing

To test their utility for PG labeling, we incubated RfDAAs with two Gram-positive species, *S. venezuelae* (15 min, 1/3 doubling time) and *B. subtilis* (1 hour, 3 doubling times), and directly imaged the cells without washing and fixation (Fig. 2a, Supplementary Fig. 2). With the short-pulse incubation, newly synthesized PG in *S. venezuelae* was clearly detected at the poles; while the long-pulse incubation in *B. subtilis* resulted in full cell wall labeling. These labeling patterns are consistent with the control samples using standard FDAA, HADA.[15–17] However, washing steps were required to remove excess dye for imaging HADA labeling. Otherwise, strong background fluorescence saturated the fluorescence signal and prevented PG imaging (Fig. 2b). In comparison, PG labeling using RfDAAs could be observed without washing steps. The specific labeling of PG with RfDAAs was confirmed by visualizing **Rf470DL** signal in isolated sacculi from *B. subtilis* (Supplementary Fig. 3). Control experiments using L-enantiomers of RfDAAs showed no significant signal under the same labeling and imaging condition, suggesting that RfDAA labeling is mediated by PG transpeptidase activity (Fig. 2b, Supplementary Fig. 2).

The outer-membrane (OM) in Gram-negative species is an effective barrier that prevents the entry of molecules from the environment.[35] To investigate the utility of RfDAAs in Gram-negative bacteria, we determined their OM permeability by performing a long-pulse labeling in wild-type *Escherichia coli* (*E. coli* WT) and a mutant with increased membrane permeability (*E. coli imp*).[36] In WT cells, no significant signal above the background was detected with all the RfDAAs (Supplementary Fig. 4). In contrast, up to a 7-fold signal increase was observed in *E. coli imp* with **Rf470DL** and **Rf490DL** (Supplementary Fig. 4). This suggested that the OM presents a substantial barrier for the labeling. Thus, permeabilizing the OM might be required to label Gram-negatives with RfDAAs. **Rf420DL** showed faint fluorescence signal even in *E. coli imp*. We wondered whether **Rf420DL** is toxic to the cells so we measured the growth curves of *E. coli imp* and *B. subtilis* in the presence of RfDAAs (Supplementary Fig. 5). It appears that all the RfDAAs are highly biocompatible in these species at 1 mM concentration. No significant growth delay was found in the RfDAA samples compared to the DMSO controls. Thus, the low labeling signal of **Rf420DL** is not due to toxicity but probably its photochemical properties (Supplementary discussion 1).

We hypothesized that the PG layer constrains the conformation of the RfDAAs, leading to fluorescence release. In further support of this, we determined the viscosity sensitivity (χ) of RfDAAs by measuring their fluorescence intensity as a function of solvent viscosity using a glycerol gradient (Table 1). All the probes have a ~20 fold intensity increase in 80% glycerol-PBS compared to pure PBS (Supplementary Fig. 6). The calculated viscosity sensitivity of RfDAAs is about 0.65, a typical value for fluorescent molecular rotors.[37,38] HADA intensity remained the same in this test with a χ value of 0.025, showing that HADA does not have molecular rotor properties. We were then interested in the viscosity sensitivity

of incorporated RfDAAs in PG structures. If the dyes inside the PG layer are sterically restricted into the “on” state, we would expect a decreased viscosity sensitivity. We prepared *B. subtilis* cells labeled with **Rf470DL** for 1 hour, followed by fixing the cells with ethanol and washing with PBS twice. The pellets were then resuspended in glycerol-PBS solution for fluorescence measurement. We found that incorporated **Rf470DL** showed significantly decreased viscosity sensitivity (χ=0.27), indicating that the molecular rotors had already achieved a highly constrained state likely due to the PG surroundings (Supplementary Fig. 6). Thus, incorporation into the cell wall is sufficient to activate the fluorescence state of RfDAAs.

Real-time imaging of PG synthesis with Rf470DL

We chose **Rf470DL** for time-lapse experiments because it possesses the highest quantum yield and absorptivity (Table 1). Cells were spotted on an LB-agarose pad containing **Rf470DL** and imaged continuously using epifluorescence microscopy (Fig. 3a). In *S. venezuelae*, a polarly growing bacterium, **Rf470DL** signal was first seen at growing poles, newly developed branches, and division septa (Fig. 3b, Supplementary Movie 1). The labeled area extended over time along with the elongation of the poles and new cell branches. The formation of new septa could be observed clearly during the time-lapse imaging. On the other hand, in *B. subtilis,* **Rf470DL** signal increased gradually throughout the cell body with the dimmest intensity at the poles (Supplementary Fig. 7, Supplementary Movie 2). This is consistent with the dispersed growth mode in this species as reported previously.[39] The formation of division septa could also be seen in real time. Thus, we conclude that RfDAAs enable real-time monitoring of PG synthesis in live cells. Since washing steps are no longer required, RfDAA labeling provides improved temporal resolution compared to sequential FDAA labeling. Interestingly, we also found that non-growing cells showed extremely strong fluorescence signal throughout the whole cell body (Supplementary Movie 3). This is probably due to membrane permeabilization in dying cells, which allows the entrance of RfDAAs into the cytoplasm, a relatively viscous environment that may turn on the probes. Thus, permeabilized and dying cells can be easily distinguished from live cells during time-lapse experiments using RfDAAs.

Real-time assays of transpeptidase activity using Rf470DL

In vitro assays to study D,D-transpeptidation activity have been developed previously and have greatly advanced our understanding of PBP kinetics as well as PG synthesis mechanisms.[4,14,40–43] However, due to the presence of strong background noise from the leftover probes, signal output in the existing transpeptidase assays can only be obtained after product purification processes. This complicates the experiments and increases the amount of human works. Given that RfDAAs are fluorogenic probes that fluoresce upon PG incorporation, we developed a continuous, spectrophotometric assay to monitor transpeptidation reactions without the need of product purification. The component of the assay includes RfDAA probes as the fluorescence reporter, synthetic diacetyl-L-lysine-D-alanine-D-alanine as the substrate (acyl donor) and *Staphylococcus aureus* PBP4 enzyme. *S. aureus* PBP4 is a known D,D-transpeptidase responsible for PG cross-linking in staphylococci, as well as a β-lactamase that degrades penicillin-like antibiotics.[44,45] Knocking out PBP4 results in significantly decreased resistance to β-lactams in methicillin-

resistant *S. aureus* (MRSA), suggesting that it is a valuable target for new antibiotic development.[46]

S. aureus PBP4 was added to a mixture of **Rf470DL** and the synthetic substrate in a 96-well plate. The fluorescence intensity of the samples was then measured over time using a plate reader (Fig. 4a). An increase in intensity was observed (Fig. 4b) and the formation of cross-linked product was confirmed by reverse-phase HPLC and high-resolution mass spectrometry (Fig. 4c, d). Control experiments using the L-enantiomer of **Rf470DL** showed no signal increase in the assay (Supplementary Fig. 8), which is in agreement with the stereocenter selectivity of PBPs. To confirm that the reaction was carried out by enzyme activity, a known effective inhibitor of *S. aureus* PBP4, cefoxitin, was added to the reaction. A total inhibition of the D,D-transpeptidation activity was observed.[46] In contrast, when chloramphenicol, a ribosome peptidyl transferase inhibitor, was added, no inhibition effect was found. These results indicated that the signal increase in the assay results from *S. aureus* PBP4 activity, and that RfDAAs could be employed for real-time monitoring of D,D-transpeptidation reaction *in vitro*. In addition, a dose-dependent experiment using cefoxitin indicated a total inhibition of *S. aureus* PBP4 activity at 5 μg/ml (estimated IC_{50}= 1 μg/ml), consistent with the reported MIC value in this species (Supplementary Fig. 9).[47]

We further evaluated the utility of this assay for high-throughput screening for antibiotics. We tested various antibiotics and measured the initial rate of fluorescence increase (Fig. 4e). As expected, antibiotics targeting the protein synthesis machinery showed no significant effect to *S. aureus* PBP4 activity; whereas β-lactam derivatives had inhibitory activities: Cefoxitin and Carbenicillin inhibited the enzyme reaction almost completely; Penicillin G and Ampicillin showed partial inhibition; and Piperacillin, a selective inhibitor of *E. coli* PBP3 [48], did not have a significant effect on *S. aureus* PBP4 activity. This result is consistent with the published inhibitory concentration of these β-lactams against *S. aureus*.[49] To further confirm the observed inhibitory effects, we performed a Nitrocefin test, which determines PBP's β-lactamase activity, in the presence of these antibiotics.[50,51] We found that, in the presence of Cefoxitin or Carbenicillin, Nitrocefin hydrolysis was strongly inhibited (> 50 %, Fig. 4f). However, Piperacillin and Ampicillin treatments did not inhibit PBP4s β-lactamase activity effectively, indicating a low inhibitory effect toward PBP4. Together, these results suggest that RfDAAs can be used to quantitatively measure the effect of β-lactams on the transpeptidation activity of PBPs. We also note that this assay can be conducted in an end-point manner, providing an efficient way to test a large number of samples since only a single measurement is required per sample (Supplementary Fig. 10).

In addition to PBPs, we tested the RfDAA assay in other classes of transpeptidases: L,D-transpeptidases (Ldts) and Sortases. It is known that LdtA, encoded by *V. cholerae vc1268*, is responsible for 3'−3' cross-linkage formation[52]. Incubation of LdtA with **Rf470DL** and a synthetic tetrapeptide (diacyl-L-Ala-D-Glu-L-Lys-D-Ala) leads to a time-lapse increase of fluorescence signal, similar to our observations in the *S. aureus* PBP4 experiments (Supplementary Fig. 11). On the other hand, *S. aureus* Sortase A (SrtA) is responsible for anchoring surface proteins to PG through a sequence-specific transpeptidation reaction[13]. It recognizes a conserved protein LPXTG motif and cross-links it with PG pentaglycine in *S. aureus*. We incubated Sortase A with synthetic pentapeptide motif (LPETG) in the RfDAA

assay and observed an increase of **Rf470DL** signal over time (Supplementary Fig. 11). Control experiments in the absence of the substrate led to no signal change. These results suggest that our *in vitro* RfDAA assay is highly applicable in transpeptidase activity measurement for studying PG-to-PG and PG-to-protein cross-linking reactions.

Discussions

Tracking PG biosynthesis during the life cycle of a bacterial cell has been a long-term challenge in the field of PG studies. Sequential PG labeling using FDAAs has a limited temporal resolution (> 15 s) due to the need of removing background fluorescence caused by the unincorporated dye.[19] Fluorogenic probes, such as RfDAAs, can match the superior temporal resolutions (< 1 s) of cutting-edge protein-tracking methods toward understanding the spatiotemporal coordination between PG synthases and PG synthesis. Since washing steps are no longer required and the cells can be imaged directly after treated to RfDAAs, the temporal resolution of RfDAA labeling is simply defined by the microscope capability and can easily achieve sub-second scale. The removal of washing steps also minimizes the perturbation to bacterial cells. These improvements would allow close tracking of PG formation that proceeds fast (e.g. PG formation in short doubling-time species) as well as simultaneous monitoring of enzyme localization versus PG growth activities (e.g. the localization of active PBPs and newly formed PG).

PG transpeptidation reactions are valuable antibiotic targets because there is no PG equivalent in eukaryotic systems, which reduces toxicity effects to human patients. *In vitro* transpeptidase assays are powerful tools for identifying new PG-specific inhibitors. However, efficient drug development cannot be achieved until low-cost, high-throughput screening methods become available. Under the mounting stress of bacterial resistance, developing such an efficient screening method becomes urgent. RfDAAs allow specific PG labeling through transpeptidase activities. Endowed by their fluorogenic properties, RfDAA assays bypass the need of staining and/or purification processes. This greatly reduces the cost and time from the current HPCL-based approaches, increasing the efficiency toward new drug screens. In addition, we show that RfDAAs can report the activities of other classes of transpeptidases, L,D-transpeptidases (LdtA, *V. cholerae*) and sortases (SrtA. *S. aureus*), that are both proposed to be new antibiotic targets with few inhibitors available.[11,13,53,54] The broad applicability of the assay also suggests that RfDAAs could be applicable to other transpeptidation reactions, such as eukaryotic transglutaminases.[55] Therefore, *in vitro* RfDAA assays could facilitate high-throughput screens toward the discovery of a variety of drug candidates.

Finally, as a prospect of future application, the turn-on behavior of RfDAAs upon incorporation into the PG stem peptide sets this class of amino acids as powerful new protein tags. The wash-free labeling of proteins with these small fluorogenic amino acids at the L-chirality using genetic code expansion could improve upon current fluorescent protein labeling technologies for most applications.[56] These probes would perturb the tagged protein minimally and would be instantly visible upon protein incorporation as they do not require maturation or oxygen to fluoresce.

To conclude, in this study, we demonstrate the use of RfDAAs, the first fluorogenic amino acids that fluoresce only upon incorporation into PG. As D-amino acid derivatives, RfDAAs label PG through PBP transpeptidation activity, therefore allowing real-time monitoring of PG synthesis *in vivo* as well as continuous transpeptidation assays *in vitro*. We show the potential of RfDAAs for studying mechanisms of PG synthesis both at the sub-cellular and enzyme kinetics level, and for high-throughput screening of novel antibacterial drugs.

Methods

For more discussions and experimental details, please refer to Electronic Supporting Information (ESI).

Supplementary Material

Refer to Web version on PubMed Central for supplementary material.

Acknowledgements

We thank Kerwyn Casey Huang for providing strain *E. coli imp4213*, Suzanne Walker for providing *S. aureus* PBP4 plasmid, David Kysela for help on image processing and analysis, and Jonathan Rittichier for providing the enzyme substrates used in the *in vitro* assays and his kind advice on RfDAA synthesis. This study is supported by NIH grants 5R01GM113172 to MSV and YVB; and R35GM122556 to YVB.

Reference

1. Typas A, Banzhaf M, Gross C. a. & Vollmer W From the regulation of peptidoglycan synthesis to bacterial growth and morphology. Nat. Rev. Microbiol 10, 123–136 (2012).
2. Egan AJF, Cleverley RM, Peters K, Lewis RJ & Vollmer W Regulation of bacterial cell wall growth. FEBS J. 284, 851–867 (2017). [PubMed: 27862967]
3. Vollmer W, Blanot D & de Pedro MA Peptidoglycan structure and architecture. FEMS Microbiol. Rev 32, 149–167 (2008). [PubMed: 18194336]
4. Lupoli TJ et al. Transpeptidase-Mediated Incorporation of D-amino acids into bacterial peptidoglycan. J. Am. Chem. Soc 133, 10748–51 (2011). [PubMed: 21682301]
5. Wilke MS, Lovering AL & Strynadka NC β-Lactam antibiotic resistance: a current structural perspective. Curr. Opin. Microbiol 8, 525–533 (2005). [PubMed: 16129657]
6. Waxman DJ & Strominger JL Penicillin-Binding Proteins and the Mechanism of Action of Beta-Lactam Antibiotics1. Annu. Rev. Biochem 52, 825–869 (1983). [PubMed: 6351730]
7. Tipper DJ & Strominger JL Mechanism of action of penicillins: a proposal based on their structural similarity to acyl-D-alanyl-D-alanine. Proc. Natl. Acad. Sci. U. S. A 54, 1133–41 (1965). [PubMed: 5219821]
8. Sauvage E, Kerff F, Terrak M, Ayala JA & Charlier P The penicillin-binding proteins: Structure and role in peptidoglycan biosynthesis. FEMS Microbiol. Rev 32, 234–258 (2008). [PubMed: 18266856]
9. Mainardi J-L et al. A novel peptidoglycan cross-linking enzyme for a beta-lactam-resistant transpeptidation pathway. J. Biol. Chem 280, 38146–52 (2005). [PubMed: 16144833]
10. Mainardi J-L et al. Novel Mechanism of β-Lactam Resistance Due to Bypass of DD-Transpeptidation in Enterococcus faecium. J. Biol. Chem 275, 16490–16496 (2000). [PubMed: 10748168]
11. Hugonnet J-E et al. Factors essential for L,D-transpeptidase-mediated peptidoglycan cross-linking and β-lactam resistance in Escherichia coli. Elife 5, (2016).

12. Mazmanian SK, Liu G, Jensen ER, Lenoy E & Schneewind O Staphylococcus aureus sortase mutants defective in the display of surface proteins and in the pathogenesis of animal infections. Proc. Natl. Acad. Sci. U. S. A. 97, 5510–5 (2000). [PubMed: 10805806]
13. Ton-That H, Liu G, Mazmanian SK, Faull KF & Schneewind O Purification and characterization of sortase, the transpeptidase that cleaves surface proteins of Staphylococcus aureus at the LPXTG motif. Proc. Natl. Acad. Sci. U. S. A 96, 12424–9 (1999). [PubMed: 10535938]
14. Egan AJF, Biboy J, van't Veer I, Breukink E & Vollmer W Activities and regulation of peptidoglycan synthases. Philos. Trans. R. Soc. B Biol. Sci 370, 20150031 (2015).
15. Kuru E et al. In Situ probing of newly synthesized peptidoglycan in live bacteria with fluorescent D-amino acids. Angew. Chem. Int. Ed. Engl 51, 12519–23 (2012). [PubMed: 23055266]
16. Kuru E, Tekkam S, Hall E, Brun YV & Van Nieuwenhze MS Synthesis of fluorescent D-amino acids and their use for probing peptidoglycan synthesis and bacterial growth in situ. Nat. Protoc 10, 33–52 (2015). [PubMed: 25474031]
17. Hsu Y-P et al. Full color palette of fluorescent d -amino acids for in situ labeling of bacterial cell walls. Chem. Sci 290, 30540–30550 (2017).
18. Hsu Y-PP, Meng X & VanNieuwenhze MSS Methods for visualization of peptidoglycan biosynthesis Methods in Microbiology 43, 3–48 (Elsevier Ltd, 2016).
19. Bisson-Filho AW et al. Treadmilling by FtsZ filaments drives peptidoglycan synthesis and bacterial cell division. Science (80-.). 355, 739–743 (2017).
20. Haidekker MA & Theodorakis EA Environment-sensitive behavior of fluorescent molecular rotors. J. Biol. Eng 4, 11 (2010). [PubMed: 20843326]
21. Haidekker MA et al. A Ratiometric Fluorescent Viscosity Sensor. J. Am. Chem. Soc 128, 398–399 (2006). [PubMed: 16402812]
22. Kuimova MK Mapping viscosity in cells using molecular rotors. Phys. Chem. Chem. Phys 14, 12671 (2012). [PubMed: 22806312]
23. Hosny NA et al. Mapping microbubble viscosity using fluorescence lifetime imaging of molecular rotors. Proc. Natl. Acad. Sci. U. S. A 110, 9225–30 (2013). [PubMed: 23690599]
24. Goh WL et al. Molecular rotors as conditionally fluorescent labels for rapid detection of biomolecular interactions. J. Am. Chem. Soc 136, 6159–62 (2014). [PubMed: 24494589]
25. Yu W-T, Wu T-W, Huang C-L, Chen I-C & Tan K-T Protein sensing in living cells by molecular rotor-based fluorescence-switchable chemical probes. Chem. Sci 7, 301–307 (2016). [PubMed: 28758005]
26. Dziuba D, Jurkiewicz P, Cebecauer M, Hof M & Hocek M A Rotational BODIPY Nucleotide: An Environment-Sensitive Fluorescence-Lifetime Probe for DNA Interactions and Applications in Live-Cell Microscopy. Angew. Chemie 128, 182–186 (2016).
27. Nadler A & Schultz C The Power of Fluorogenic Probes. Angew. Chemie Int. Ed 52, 2408–2410 (2013).
28. Kamariza M et al. Rapid detection of Mycobacterium tuberculosis in sputum with a solvatochromic trehalose probe. Sci. Transl. Med 10, eaam6310 (2018). [PubMed: 29491187]
29. Haidekker MA et al. New fluorescent probes for the measurement of cell membrane viscosity. Chem. Biol 8, 123–31 (2001). [PubMed: 11251287]
30. Sawada S, Iio T, Hayashi Y & Takahashi S Fluorescent rotors and their applications to the study of G-F transformation of actin. Anal. Biochem 204, 110–7 (1992). [PubMed: 1514677]
31. De K, Legros J, Crousse B & Bonnet-Delpon D Solvent-promoted and -controlled aza-Michael reaction with aromatic amines. J. Org. Chem 74, 6260–5 (2009). [PubMed: 19621888]
32. Shao J et al. Thiophene-Inserted Aryl-Dicyanovinyl Compounds: The Second Generation of Fluorescent Molecular Rotors with Significantly Redshifted Emission and Large Stokes Shift. European J. Org. Chem 2011, 6100–6109 (2011).
33. Monnereau C, Blart E & Odobel F A cheap and efficient method for selective para-iodination of aniline derivatives. Tetrahedron Lett. 46, 5421–5423 (2005).
34. Suzuki A Recent advances in the cross-coupling reactions of organoboron derivatives with organic electrophiles, 1995–1998. J. Organomet. Chem 576, 147–168 (1999).

35. Delcour AH Outer membrane permeability and antibiotic resistance. Biochim. Biophys. Acta - Proteins Proteomics 1794, 808–816 (2009).
36. Sampson BA, Misra R & Benson SA Identification and characterization of a new gene of Escherichia coli K-12 involved in outer membrane permeability. Genetics 122, 491–501 (1989). [PubMed: 2547691]
37. Zhou F et al. Molecular Rotors as Fluorescent Viscosity Sensors: Molecular Design, Polarity Sensitivity, Dipole Moments Changes, Screening Solvents, and Deactivation Channel of the Excited States. European J. Org. Chem 2011, 4773–4787 (2011).
38. Haidekker MA et al. Molecular rotors—fluorescent biosensors for viscosity and flow. Org. Biomol. Chem 5, 1669–1678 (2007). [PubMed: 17520133]
39. Randich AM & Brun YV Molecular mechanisms for the evolution of bacterial morphologies and growth modes. Front. Microbiol 6, 1–13 (2015). [PubMed: 25653648]
40. Lupoli TJ et al. Lipoprotein Activators Stimulate Escherichia coli Penicillin-Binding Proteins by Di ff erent Mechanisms. J. Am. Chem. Soc 136, 52–55 (2014). [PubMed: 24341982]
41. Bertsche U, Breukink E, Kast T & Vollmer W In Vitro Murein (Peptidoglycan) Synthesis by Dimers of the Bifunctional Transglycosylase-Transpeptidase PBP1B from Escherichia coli. J. Biol. Chem 280, 38096–38101 (2005). [PubMed: 16154998]
42. Born P, Breukink E & Vollmer W In Vitro Synthesis of Cross-linked Murein and Its Attachment to Sacculi by PBP1A from Escherichia coli. J. Biol. Chem 281, 26985–26993 (2006). [PubMed: 16840781]
43. Qiao Y et al. Lipid II overproduction allows direct assay of transpeptidase inhibition by β-lactams. Nat. Chem. Biol 13, 793–798 (2017). [PubMed: 28553948]
44. Navratna V et al. Molecular basis for the role of Staphylococcus aureus penicillin binding protein 4 in antimicrobial resistance. J. Bacteriol 192, 134–144 (2010). [PubMed: 19854906]
45. Wyke AW, Ward JB, Hayes MV & Curtis NA A role in vivo for penicillin-binding protein-4 of Staphylococcus aureus. Eur. J. Biochem 119, 389–93 (1981). [PubMed: 7308191]
46. Memmi G, Filipe SR, Pinho MG, Fu Z & Cheung A Staphylococcus aureus PBP4 is essential for β-lactam resistance in community-acquired methicillin-resistant strains. Antimicrob. Agents Chemother 52, 3955–3966 (2008). [PubMed: 18725435]
47. Swenson JM et al. Correlation of cefoxitin MICs with the presence of mecA in Staphylococcus spp. J. Clin. Microbiol 47, 1902–5 (2009). [PubMed: 19357210]
48. Kocaoglu O & Carlson EE Profiling of β-lactam selectivity for penicillin-binding proteins in Escherichia coli strain DC2. Antimicrob. Agents Chemother 59, 2785–90 (2015). [PubMed: 25733506]
49. Wehrli R, von Graevenitz A & Lüthy R Susceptibility and tolerance of β-lactamase-producing, methicillin-sensitive strains of Staphylococcus aureus towards seven broad-spectrum penicillins. Infection 11, 322–325 (1983). [PubMed: 6607889]
50. Uri JV Detection of beta-lactamase activity with nitrocefin of multiple strains of various microbial genera. Acta Microbiol. Hung 32, 133–45 (1985). [PubMed: 3933272]
51. Pitkälä A, Salmikivi L, Bredbacka P, Myllyniemi A-L & Koskinen MT Comparison of tests for detection of beta-lactamase-producing staphylococci. J. Clin. Microbiol 45, 2031–3 (2007). [PubMed: 17428938]
52. Cava F, de Pedro MA, Lam H, Davis BM & Waldor MK Distinct pathways for modification of the bacterial cell wall by non-canonical D-amino acids. EMBO J. 30, 3442–3453 (2011). [PubMed: 21792174]
53. Guo Y, Cai S, Gu G, Guo Z & Long Z Recent progress in the development of sortase A inhibitors as novel anti-bacterial virulence agents. RSC Advances 5, 49880–49889 (2015).
54. Oh K-B et al. Discovery of Diarylacrylonitriles as a Novel Series of Small Molecule Sortase A Inhibitors. J. Med. Chem 47, 2418–2421 (2004). [PubMed: 15115384]
55. Lorand L & Graham RM Transglutaminases: Crosslinking enzymes with pleiotropic functions. Nature Reviews Molecular Cell Biology 4, 140–156 (2003). [PubMed: 12563291]
56. Kunjapur AM et al. Engineering posttranslational proofreading to discriminate nonstandard amino acids. Proc. Natl. Acad. Sci. U. S. A 115, 619–624 (2018). [PubMed: 29301968]

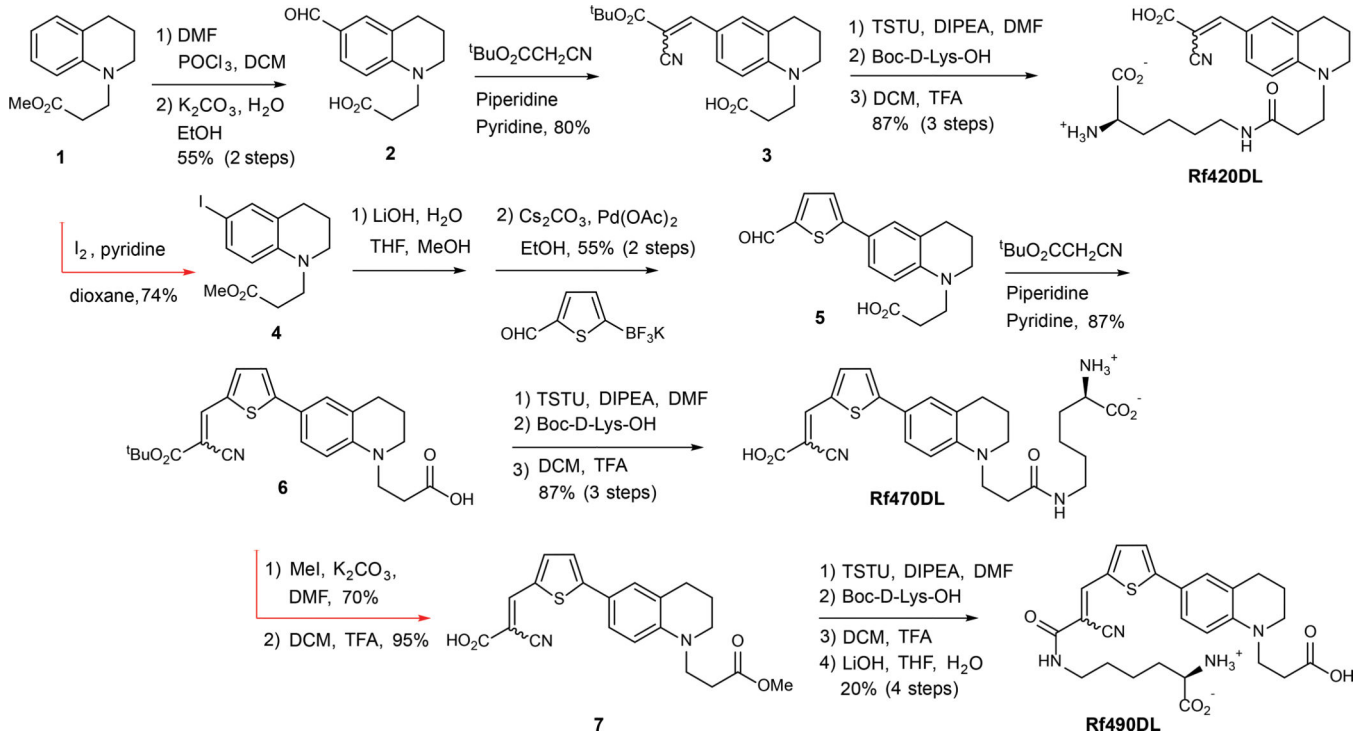

Figure 1. Synthetic routes for preparation of the RfDAAs.

Each synthetic route utilized an alkylated tetrahydroquinoline core structure (**1**) that incorporated an ester group to provide a functional handle for subsequent D-amino acid coupling. After Vilsmeier-Haack formylation, condensation with *t*-butyl cyanoacetate provided the fluorogenic fluorophore, Rf420 (**3**), which was coupled with D-Lys to generate **Rf420DL**. A similar strategy was used to prepare **Rf470DL**. A thiophene spacer, installed via iodination of the aryl ring and a subsequent Suzuki-Miyaura coupling reaction, was added to the tetrahydroquinoline core in order to further extend conjugation (e.g., **6**). **Rf490DL**, a constitutional isomer of **Rf470DL**, was prepared by coupling D-Lys to the deprotected α-cyanoacrylic acid subunit (**7**).

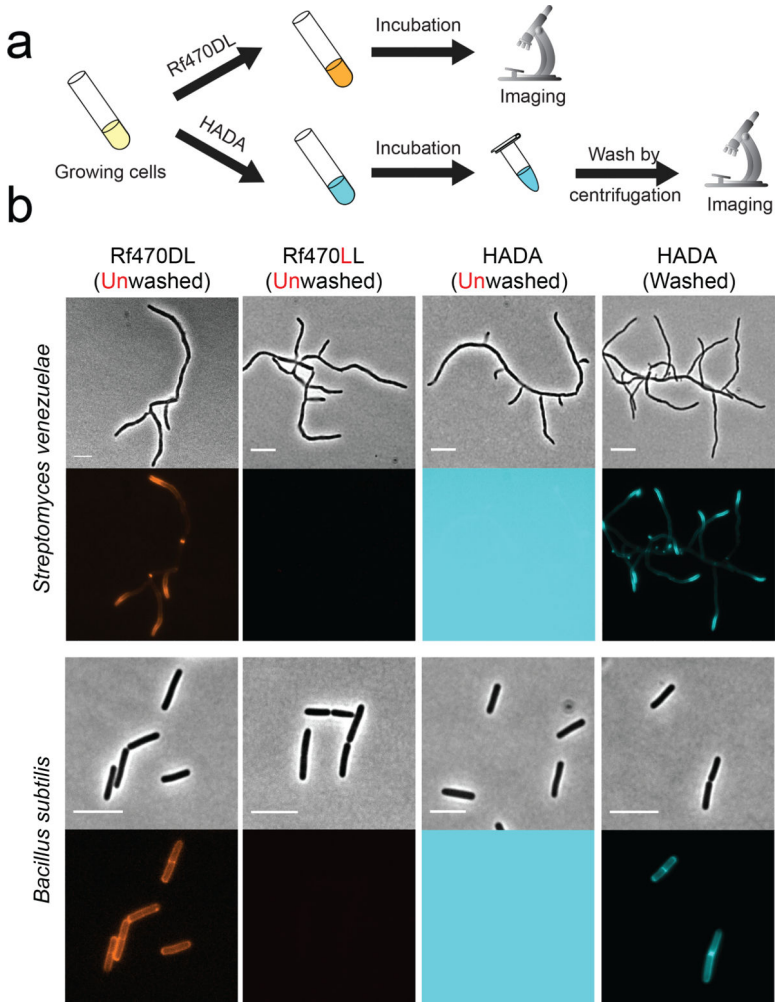

Figure 2. Unlike FDAAs, RfDAAs allow wash-free imaging of bacterial cell walls.

a) Scheme of labeling process. Bacterial cells were incubated with either RfDAAs or FDAA for PG labeling. The labeled cells were then collected and imaged with or without washing steps. b) Cell images shown in phase contrast (upper row) and fluorescence (bottom row) channels. Top panel: short-pulse labeling in *S. venezuelae* (1/3 doubling time); bottom panel: long-pulse labeling in *B. subtilis* (3 doubling times). PG labeling using RfDAAs (red) can be imaged without washing steps; whereas FDAA labeling (cyan) before washing steps results in saturated background fluorescence due to excess FDAAs in the field of view. Identical labeling, imaging and processing protocols were used for the comparison between D- and L- enantiomer labeling, as well as for unwashed and washed HADA labeling. Scale bar: 5 μm.

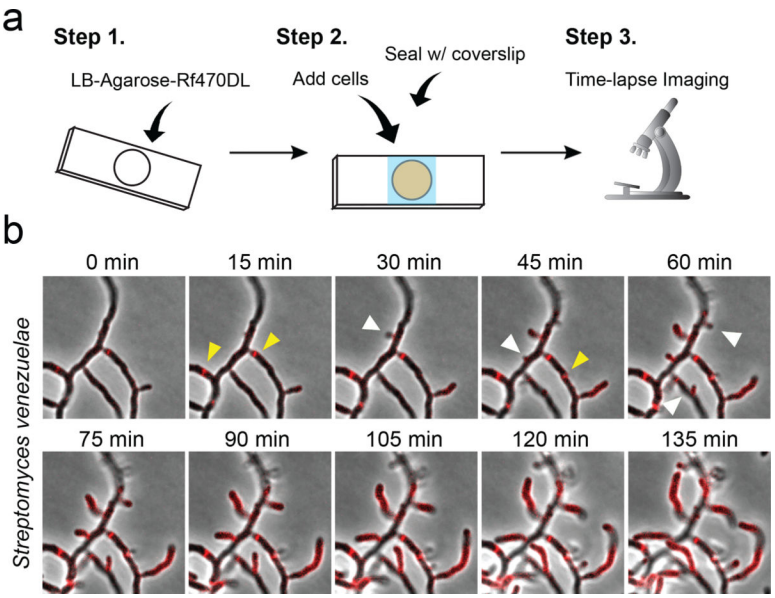

Figure 3. RfDAAs allow real-time imaging of PG synthesis in *S. venezuelae*.

a) Scheme of labeling process. Pre-warmed liquid mixture of LB-agarose and **Rf470DL** was added to a cavity slide. After the mixture was solidified, cells were loaded on top of the agarose pad and then covered with a coverslip. Real-time PG labeling was then observed using time-lapse fluorescence microscopy while the cells were growing in the slides. b) Montage image of **Rf470DL** time-lapse labeling in *S. venezuelae.* Newly synthesized PG structures are revealed by the appearance of new **Rf470DL** signal (red). The extension of peripheral PG, the formation of septal PG and the formation of new cell branches are revealed by the **Rf470DL** signal over time. Yellow arrowheads: newly formed septal PG; white arrowhead: newly formed cell branches. See Supplementary Movie 1. Scale bar: 5 μm.

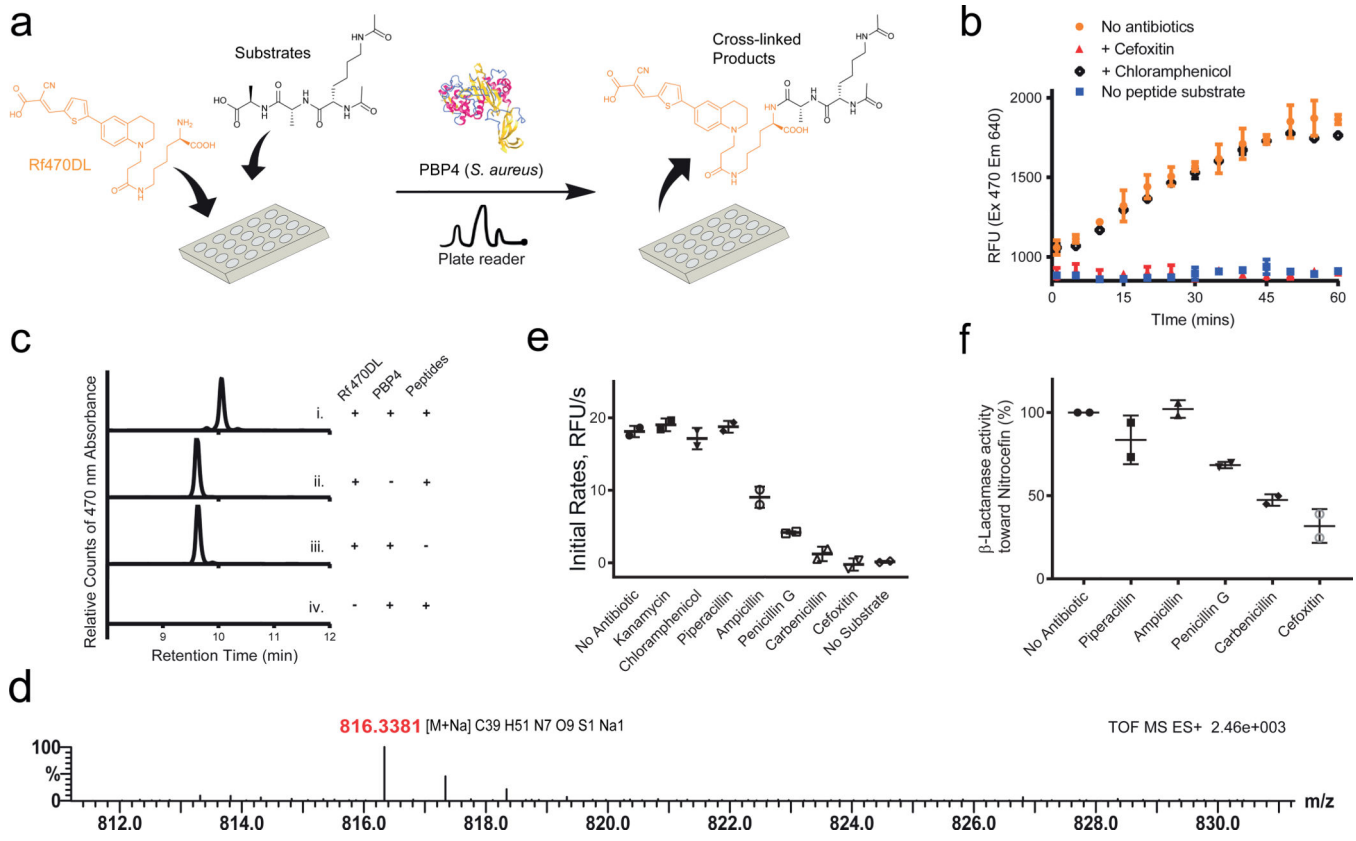

Figure 4. RfDAAs facilitate real-time *in vitro* transpeptidation assays.

a) Scheme of assay procedure. **Rf470DL** and the synthetic substrate were mixed in a 96-well plate. The fluorescence intensity of **Rf470DL** was then measured over time upon the addition of recombinant *S. aureus* PBP4. b) Real-time monitoring of **Rf470DL** intensity. An intensity increase was observed in the assay; while adding PBP inhibitors blocked the reaction. c) HPLC analysis of the assay products. A shifted retention time was observed when the **Rf470DL**-substrate mixture was treated with PBP4. d) High-resolution MS analysis of the products from the assay confirmed the formation of the cross-linked product. e) Screening of antibiotic effect on *S aureus* PBP4 activity. A 1:10 ratio of antibiotics to the substrate was used in the experiments. Kanamycin and Chloramphenicol (ribosome inhibitors) did not inhibit the **Rf470DL** incorporation. Piperacillin, Ampicillin, Penicillin G, Carbenicillin and Cefoxitin (β-lactam antibiotics) showed different level of inhibition. f) β-lactamase activity of *S. aureus* PBP4. A competition assay using Nitrocefin was performed to study PBP4 β-lactamase activity toward the β-lactam antibiotics used in the assay experiments. In this panel, low activity stands for a strong inhibition effect of the antibiotics toward PBP4, and vice versa. Values are normalized to the “no antibiotic” sample. Error bars: Mean value and standard deviation.

Table 1.

Photochemical and physical properties of RfDAAs.

	Rf420DL	Rf470DL	Rf490DL	HADA
MW (unsalted)	428.5	510.6	510.6	292.1
Max. λ_{Ex} [a]	420	470	490	400
Max. λ_{Em} [a]	490	640	660	450
Viscosity sensitivity (X)	0.683±0.013	0.642±0.022	0.670±0.003	0.025±0.003
Quantum Yield (ϕ) [a,b]	0.012	0.042	0.035	NA
Absorptivity (ε) [c]	19761	33106	25409	109538
Water-solubility ($LogD_{7.4}$) [d]	−1.497±0.045	−1.150±0.09	−1.10±0.07	−1.059±0.076
Thermo-stability [c,e]	99.8±1.2%	99.4±1.4%	96.9±9.8%	80.0±1.1%

[a] Data were measured in PBS (pH 7.4) containing 50% glycerol.

[b] Fluorescein was used as a standard for quantum yield measurements.

[c] Data were measured in PBS (pH 7.4).

[d] Data were measured using a PBS (pH 7.4) and 1-octanol extraction. A smaller value represents greater water solubility.

[e] Value represents signal retention of absorbance after a 24-hours incubation at 60 °C compared to the corresponding initial value.